LA-UR -84-2764

CONF-8406158--3

LA-UR--84-2764

DE85 002010

TITLE: PRELIMINARY RESULTS OF ν_ee- SCATTERING AT LAMPF

AUTHOR(S): R. C. Allen, V. Bharadwaj, G. A. Brooks, H. H. Chen, P. J. Doe, R. Hausammann, H. J. Mahler, A. M. Rushton, K. C. Wang, T. J. Bowles, R. L. Burman, R. D. Carlini, D. R. F. Cochran, J. S. Frank, E. Piasetzky, V. D. Sandberg, D. A. Krakauer, and R. C. Talaga

SUBMITTED TO: Neutrino '84 Conference, Dortmund, Federal Republic of Germany, June 1984.

Los Alamos

Los Alamos National Laboratory
Los Alamos, New Mexico 87545

FORM NO 836 R4
ST NO 2629 5/81

UCI-Neutrino No. 122
August, 1984

PRELIMINARY RESULTS OF ν_e e^- SCATTERING AT LAMPF

R. C. Allen, V. Bharadwaj,[a] G. A. Brooks,[b]
H. H. Chen, P. J. Doe, R. Hausammann,[c]
H. J. Mahler, A. M. Rushton,[d] K. C. Wang,

University of California, Irvine, California 92717

T. J. Bowles, R. L. Burman, R. D. Carlini,
D. R. F. Cochran, J. S. Frank, E. Piasetzky,
V. D. Sandberg,

Los Alamos National Laboratory, Los Alamos,
New Mexico 87545

D. A. Krakauer, and R. C. Talaga

University of Maryland, College Park, Maryland 20742

ABSTRACT

We present preliminary results of a neutrino experiment in progress at LAMPF by an Irvine-Los Alamos-Maryland collaboration. We have observed a signal consistent with ν_e e^- elastic scattering, with a 15-ton sandwich detector. The number of these ν_e e^- candidates agrees with that predicted by the Weinberg-Salam electroweak theory. The corresponding $\sin^2\theta_W$ and total cross section are reported. This study shows that the interference of weak charged-current and weak neutral-current in ν_e e^- scattering is not constructive. We also searched for anomalous appearance of $\bar{\nu}_e$ from the LAMPF beam stop. An upper limit for the multiplicative lepton number conservation law, and limits for $\bar{\nu}_\mu \rightarrow \bar{\nu}_e$ oscillation are given.

1. Introduction

The study of purely leptonic processes such as neutrino-electron elastic scattering can provide stringent tests on the validity of the Weinberg-Salam (W-S) electroweak theory.[1-4] $\nu_\mu e^-$ and $\bar{\nu}_\mu e^-$ scatterings are being studied at high energy accelerators.[5-6] $\bar{\nu}_e e^-$ scattering was investigated in a reactor experiment.[7] It is the goal of this experiment to study $\nu_e e^-$ scattering which has not been observed before. In $\nu_e e^-$ (and $\bar{\nu}_e e^-$) scattering both weak charged-current (CC) and neutral-current (NC) interactions are involved. An accurate measurement of the $\nu_e e^-$ cross section can not only prove the existence but also determine the sign of the interference of CC and NC.[8]

At the LAMPF beam stop, ν_μ, $\bar{\nu}_\mu$, and ν_e are produced from π^+ decay at rest, followed by μ^+ decay at rest. Production of $\bar{\nu}_e$ is highly suppressed ($\leq 10^{-3}$) due to the absorption of π^- and μ^- by nuclei in the beam stop. Looking for $\bar{\nu}_e$'s from a beam stop allows one to search for anomalous $\bar{\nu}_e$ production modes such as $\bar{\nu}_\mu \rightarrow \bar{\nu}_e$ oscillation or $\mu^+ \rightarrow e^+ \bar{\nu}_e \nu_\mu$ allowed by the multiplicative lepton number conservation law.[9]

In this paper we describe our experimental method, data analysis, Monte-Carlo simulation, preliminary results, and current plans.

2. Experimental Method

The signal of elastic scattering reaction

$$\nu + e^- \rightarrow \nu + e^- \qquad (1)$$

is a recoil electron with energy less than the maximum neutrino energy (52.8 MeV) in the forward 10° cone as required by kinematics. Scattering from different types of neutrinos are not distinguishable in our detector. However, due to the presence of the CC interaction, $\nu_e e^-$ scattering dominates and the small contributions from $\nu_\mu e^-$ and $\bar{\nu}_\mu e^-$ can be subtracted by using the results of experiments from high energy accelerators. We search for $\bar{\nu}_e$'s via the appearance of e^+ from

$$\bar{\nu}_e + p \rightarrow n + e^+. \qquad (2)$$

Backgrounds come from cosmic ray muons and neutrals, and beam associated neutrals and neutrinos. For example, stopped muon decay, Compton scattering, and $\nu_e + C^{12}$ interaction can mimic signals of interest. Such backgrounds need to be highly suppressed for this study.

The detector system consists of a central sandwich detector surrounded by active anti-coincidence counters and inert shields. The central detector, weighing a total of 15 tons, is divided into 40 layers. Each layer consists of a plane of plastic scintillator (for energy and timing information) and a flash chamber module (FCM) (for tracking information). A scintillation plane is constructed of 4 slabs, 2.54cm thick and viewed by a 5-inch PMT, placed side by side to give a total size of 305cm x 305cm. The scintillator system and its associated electronics was described in Ref. 10. Each FCM consists of 5 x-planes and 5 y-planes. One such plane contains 520 flash tubes (0.5cm x 0.5cm x 305cm in size). There are a total of more than 200,000 tubes in the whole detector. Operation of the FCM was described in detail in Ref. 11.

The active anti consists of about 600 Multi-Wire Proportion Counters (MWPC). All sides of the central detector are covered by 4 layers of counters, except for the single layer on the floor. Coincidence of any 2 out of these 4 layers from any side generates a valid veto signal which blocks the detector system for 20 μs. The anti inefficiency is less than 10^{-4}. There is a 14 cm steel shield against gamma-rays between the central detector and the active anti, except for the floor. Outside the MWPC's there is a 6.3 m steel shield against radiation from beam stop, and 0.6-1.8 m steel equivalent to shield against cosmic rays.

The trigger requirement was that at least 3 contiguous scintillators in 3 adjacent layers had an approximate energy deposit between 1 and 16 MeV, with the middle plane above 3 MeV, and that no valid veto existed. Duty factor of the LAMPF accelerator was 6-9%. The beam macro-pulse rate was 80-120 Hz. Data was taken with beam, and also in between beam pulses for the cosmic ray background subtraction. The trigger rate was about 0.1 per live second. For each trigger, we recorded not only the trigger event but also events 32 μs before and 64 ms after the trigger for tagging of stopped muons and $\nu_e + C^{12}$ events respectively. Totally, 127.3 hours of beam-on data and 603.3 hours of beam-off data from LAMPF Run Cycles 38-40 were taken and analyzed. The ratio of beam off/on time is 4.74.

There were 2.2 x 10^{22} protons on the beam stop for this data. During the data-taking period, we also recorded stopped muon and through muon events every 10 minutes for calibration. About 270K events were recorded on magnetic tape from these three run cycles.

3. Data Analysis

As described below, we implemented several levels of cuts to this data to search for $\nu_e\, e^-$ scattering and $\bar{\nu}_e$ p reaction.

At Cut Level 1, the calibration events were removed. There were 55K beam-on events and 203K beam-off events left. At Cut Level 2, we required the events to be totally contained in the fiducial volume, defined as Layers 2-39, and more than 5 cm from edges. We also required a single track in both views, total observable energy in scintillators ≤ 60 MeV, number of layers involved in trigger ≤ 7. In addition, no pretrigger activity in the vicinity of the trigger event was allowed. By this procedure, the total number of events was reduced by about a factor of 10.

At Cut Level 3 we required that the number of groups of activities recorded by scintillators to be 1 in order to remove neutron and gamma backgrounds. Energy cuts were implemented to select electron events. These included dE/dx ≤ 8 MeV, ΔE(end slab) ≥ 2 MeV, ΔE(middle slab) ≥ 2.5 MeV, and total observable energy in 7-35 MeV. Tighter anti cuts than the on-line veto were required to further reduce the background. These included: no adjacent anti counters in the same layer fired during the 1.2 μs in coincidence with the trigger ("in time"), no single anti signal "in time" for some anti counters around weak ones, and no floor anti activity "in time". The number of scintillator layers of trigger events is required to be ≥ 4, to decrease the sensitivity to beam-associated neutron induced events. These series of cuts reduced the number of events by about a factor of 30.

Fig. 1 shows the histogram of $\cos\theta_e$ for the remaining beam-on events and normalized (live time ratio of 4.74) beam-off events. θ_e is the recoil angle of e^- relative to the direction of the incident neutrino. In the forward angular range ($\cos\theta_e \to 1.$), the signal to cosmic ray background ratio is about 1 to 1. There are 24.2 ± 6.6 beam-on excess events in the forward angular range of $.96 \leq \cos\theta_e$ (or $\theta_e \leq 16^\circ$). The 16° cut was chosen to include $\nu_e e^-$ kinematics, multiple scattering, and detector resolution.

Beam associated background was determined by extrapolation from beam-on excess in the $\cos\theta_e$ range between 0.86 and 0.96, assuming a constant background. We attribute the remaining signal of 20.3 ± 7.3 events to neutrino (ν_e, ν_μ, and $\bar{\nu}_\mu$) electron elastic scattering.

At Cut Level 4 we subtracted the events in the forward 16° cone, and selected those with total observable energy between 23 and 33 MeV. This was done to search for the $\bar{\nu}_e p$ reaction. The number of beam-on excess events in this case is 3.7 ± 8.8.

4. Monte-Carlo Simulation and Detection Efficiency

A Monte-Carlo simulation of the detector was developed so that the response of the detector to electrons could be understood. The code was based on EGS3 (Electron Gamma Shower)[12]. EGS3 included radiative energy loss, multiple scattering, and production of secondaries from photon conversion. The straggling of energy loss, i.e. Landau Distribution,[13] was not included. The Monte-Carlo simulation took into account light attenuation in scintillators, PMT photo-electron statistics, on-line trigger requirement, and most of the cuts described above. Cuts which were left out of the Monte-Carlo were the anti cuts, the pretrigger cut, and the single track requirement. The effect of these cuts was estimated from the calibration events (both through muon and stopped muon decay).

Using W-S theory, the expected number of $\nu_e e^-$, $\nu_\mu e^-$, and $\bar{\nu}_\mu e^-$ events was calculated as a function of $\sin^2\theta_W$. In the $\nu_e e^-$ scattering case, calculations based on constructive NC and CC interference, and no interference were also carried out. The $\bar{\nu}_e p$ detection efficiency was also calculated. The uncertainty of these calculations was estimated to be 8% due to the neglect of energy loss straggling, uncertainties in the material composition, and energy calibration. Furthermore, due to the 12% uncertainty in the neutrino flux and a 10% uncertainty in the efficiency for those cuts which were not simulated by Monte-Carlo, the overall systematic uncertainty is 18%.

A comparison of the calculated and measured $\cos\theta'_e$ distributions for stopped muon events is shown in Fig. 2. Here θ'_e is measured in the lab coordinate frame. This agreement provides confidence in the Monte-Carlo simulation.

5. Preliminary Results

The observed 20.3 ± 7.3 candidates for neutrino electron scattering contain $\nu_e e^-$, $\nu_\mu e^-$, and $\bar{\nu}_\mu e^-$ components. The expected numbers of $\nu_\mu e^-$ and $\bar{\nu}_\mu e^-$ scattering were calculated to be 0.7 ± 0.2 and 2.6 ± 1.1 respectively, using the world average of measured cross sections.[14] The remaining 17.0 ± 7.4 events are $\nu_e e^-$ candidates. This number of events is consistent with W-S model with

$$\sin^2\theta_W = 0.27 \begin{matrix} +0.17 \\ -0.18 \end{matrix} \qquad (3)$$

and gives a $\nu_e e^-$ cross section of

$$\sigma(\nu_e e^-) = 10.6 \pm 4.6(\mathrm{sta.}) \pm 1.9(\mathrm{sys.}) \times E_\nu(\mathrm{GeV}) \times 10^{-42}\ \mathrm{cm}^2 \qquad (4)$$

The W-S model predicts a destructive interference between NC and CC. Table 1. shows a comparison of the observed number of $\nu_e e^-$ candidates with calculated ones with destructive (W-S), no, and constructive interference, assuming a world average $\sin^2\theta_W$ of 0.22.[14] This measurement does not agree with the constructive interference by 2.4 σ. Thus, the constructive interference is ruled out with a confidence level (CL) greater than 95%.

Table 1. Comparison of number of measured $\nu_e e^-$ scattering candidates with calculation.

(1) Measured	17.0 ± 7.4
(2) Destructive (W-S)	15.0 ± 2.7
(3) No Interference	30.8 ± 5.5
(4) Constructive	43.5 ± 7.8

If all $\bar{\nu}_\mu$'s were $\bar{\nu}_e$'s, we should have seen 801 ± 133 $\bar{\nu}_e$ p events in the range of observable energy as discussed before. However, the data contained only 3.7 ± 8.8 events. From this, we set a new upper limit of 2.2% (90% CL) for the multiplicative lepton number conservation law. As for $\bar{\nu}_\mu \rightarrow \bar{\nu}_e$ oscillation, this sets a lower limit (90% CL) of 4.4% at large Δm^2 and a lower limit of 0.61 eV^2 at $\sin^2 2\theta = 1$.

6. Present Plans

We plan to continue data taking whenever beam is available at LAMPF through 1986. By then, we expect to quadruple our data sample.

We plan to replace a steel block approximately 1 m^3 adjacent to the beam stop by uranium metal, and to improve the local shielding below the beam stop. This will reduce our beam associated background. Once these improvements are implemented, we may be able to relax the requirement of 4 scintillator layers back to 3. Then, the detection efficiency of $\nu_e e^-$ scattering can be increased by more than a factor of 2.

We plan to implement in our Monte-Carlo calculation the Landau Distribution. We are also planning to carry out a neutrino source calibration experiment with an instrumented LAMPF beam stop by measuring the number of stopped π^+ decays per incident proton.[15] These efforts will help reduce the systematic uncertainties described earlier.

7. Acknowledgments

This experiment has received much support from both the University of California, Irvine and the Los Alamos National Laboratory. We thank M. Bander, J. Brown, G. Keyworth, F. Reines, L. Rosen, and many others at both institutions for their efforts on our behalf. This project is supported by the U.S. Department of Energy and by the National Science Foundation.

8. References

(a) Present address: Fermilab, Batavia, IL 60510

(b) Present address: Saint Luke's Hospital, Houston, TX.

(c) Present address: University of Geneva, Geneva, Switzerland.

(d) Present address: DESY, D-2000, Hamburg 52, W. Germany.

1. S. Weinberg, Phys. Rev. Lett. 19, 1264 (1967).
2. G. 't Hooft, Nucl. Phys. B35, 167 (1971).
3. S. L. Glashow, Nucl. Phys. 22, 579 (1961).
4. A. Salam and J. C. Ward, Phys. Lett. 13, 168 (1964).
5. BNL Exp. 734.
6. CERN CHARM and CHARM II experiments.
7. F. Reines, H. S. Gurr, and H. W. Sobel, Phys. Rev. Lett. 37, 315 (1976).
8. B. Kayser, E. Fischbach, S. P. Rosen, and H. Spivack, Phys. Rev. D20, 87 (1979).
9. G. Feinberg and S. Weinberg, Phys. Rev. Lett. 6, 381 (1961); E. Derman, Phys. Rev. D19, 317 (1979).
10. K. C. Wang and H. H. Chen, IEEE Trans. Nucl. Sci. NS28, 405 (1981).
11. R. C. Allen, G. A. Brooks, and H. H. Chen, IEEE Trans. Nucl. Sci. NS28, 487 (1981).
12. R. L. Ford and W. R. Nelson, internal report, SLAC-210, UC-32, (1978)
13. L. Landau, J. Phys. U.S.S.R. 8, 201 (1944).
14. M. Murtagh, Neutrino '84 talk, 1984.
15. LAMPF Exp. 866.

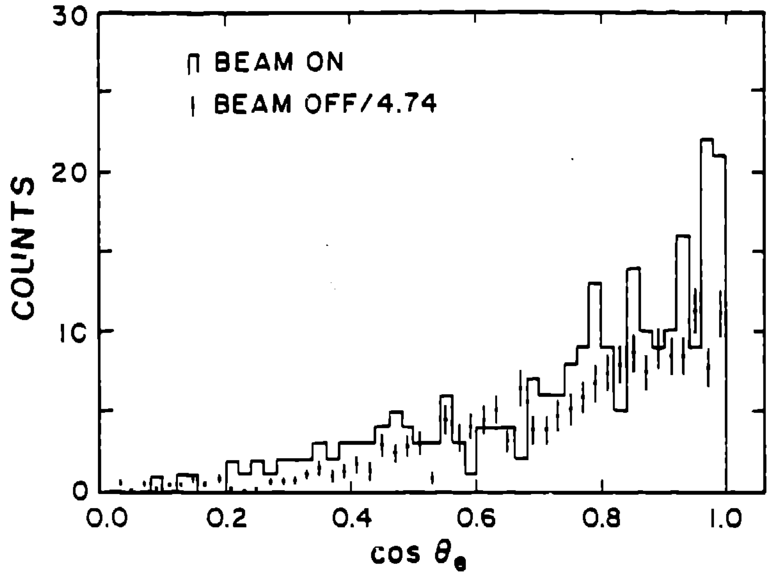

Fig. 1. Histograms of $\cos\Theta_e$ for the beam-on and normalized (live time ratio of 4.74) beam-off events after Cut Level 3. Errors for beam-off are shown. Errors for beam-on are just square root of the number of counts.

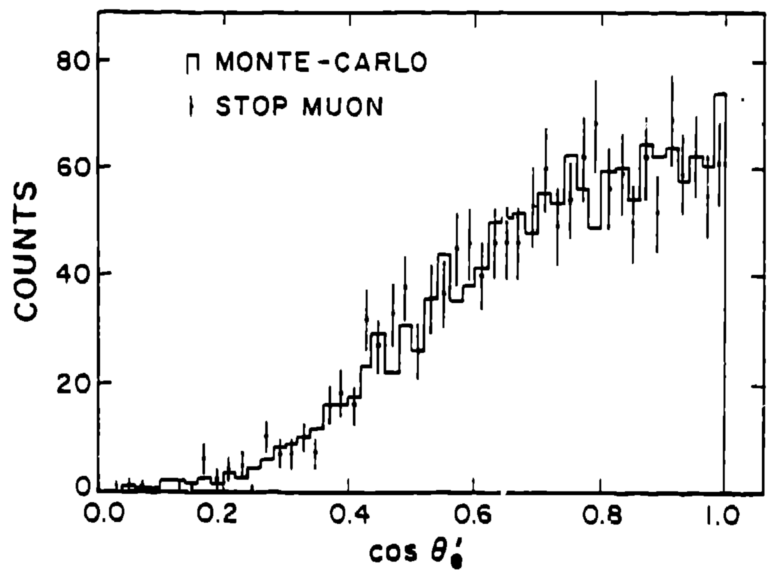

Fig. 2. Calculated and measured $\cos\theta'_e$ distributions for e^+'s from stopped muon decay. Dots with error bars are measured ones.